

Wideband perfect light absorber at midwave infrared using multiplexed metal structures

Joshua Hendrickson,¹ Junpeng Guo,^{2,*} Boyang Zhang,² Walter Buchwald,³ and Richard Soref⁴

¹Sensors Directorate, Air Force Research Laboratory, Wright Patterson Air Force Base, Ohio 45433, USA

²Department of Electrical and Computer Engineering, University of Alabama in Huntsville, Huntsville, Alabama 35899, USA

³Solid State Scientific Corporation, Nashua, New Hampshire 03060, USA

⁴Department of Physics and Engineering Program, University of Massachusetts at Boston, Boston, Massachusetts 02125, USA

*Corresponding author: guoj@uah.edu

Received October 28, 2011; accepted November 27, 2011;
posted December 9, 2011 (Doc. ID 157305); published January 24, 2012

We experimentally demonstrate a wideband near-perfect light absorber in the midwave IR region using a multiplexed plasmonic metal structure. The wideband near-perfect light absorber is made of two different size gold metal squares multiplexed on a thin dielectric spacing layer on top of a thick metal layer in each unit cell. We also fabricate regular nonmultiplexed structure perfect light absorbers. The multiplexed structure IR absorber absorbs more than 98% of the incident light over a much wider spectral band than regular nonmultiplexed structure perfect light absorbers in the midwave IR region. © 2012 Optical Society of America

OCIS codes: 160.3918, 260.3910, 240.6680.

Anomalous light absorption in metal structures was first observed a century ago by R. W. Wood [1]. The interest of light absorption in structured metals resurfaced in the 1960s, 1970s, and 1990s [2–6]. Today, it is well understood that anomalous light absorption in metal structures is due to the excitation of surface plasmon polaritons. Recently, perfect electromagnetic energy absorptions in structured metamaterials have been demonstrated in the gigahertz and terahertz regimes [7–8]. Perfect absorbers at optical frequencies have also been investigated by several groups [9–15]. However, the metamaterial perfect absorbers reported have very narrow spectral widths limited by the linewidths of the electromagnetic resonances in the structures. In many applications, it is desirable to have perfect absorptions over broad spectral bands. Expansion of the absorption spectral band has been proposed by using multiplexed subwavelength metal structures [16,17]; however, the proposed wideband absorbers have not been demonstrated. In this Letter, we report an experimental demonstration of a wide spectral band perfect light absorber in the midwave IR using a multiplexed metal structure. In the multiplexed structure, two gold metal squares are multiplexed in the unit cell of the subwavelength periodic structure. The multiplexed structure metamaterial, operating in the midwave IR regime, near-perfectly absorbs photons in the IR range over a wider spectral range than previously reported.

Figure 1(a) shows the regular nonmultiplexed perfect light absorber structure. In this structure, gold thin-film squares are periodically patterned on the top of a thin dielectric layer deposited on top of a thick gold metal layer. The thick gold layer is thick enough that no transmission can occur when light is incident from above the structure. Because of electromagnetic resonance in the metal–dielectric subwavelength structure, optical reflections from the surface can be completely eliminated when the structured surface is designed properly. Figure 1(b) shows the multiplexed perfect light absorber structure. The period of the multiplexed structure is the same as the period of the nonmultiplexed perfect light absorber structure. However, in the multiplexed struc-

ture there are two metal squares of different sizes in the unit cell. Because of the size difference, two surface plasmon resonance modes at different frequencies can occur. In both of these structures, IR transparent magnesium fluoride (MgF_2) was chosen as the dielectric spacing layer. The periods of the unit cells are identical in both lateral dimensions to insure polarization independence at the normal incidence.

We designed the regular nonmultiplexed perfect light absorbers and the multiplexed perfect light absorber in the midwave IR region. The design simulations were carried out using finite-difference time-domain software (Lumerical Solutions, Inc.). A Lorentz–Drude material model based on measurement data was used for the electric permittivity of the gold film [18]. The optical constant of the magnesium fluoride was obtained from [19]. The simulation domain has periodic boundary conditions in the lateral directions. In the directions of propagation and reflection, the simulation domain is terminated with perfect matching layers. We first carried out geometrical parameter optimization for the gold square sizes and the MgF_2 spacing layer thickness to minimize the power reflections from the nonmultiplexed and multiplexed structure absorbers for normal incidence. Figure 2 shows the calculated power reflections from two nonmultiplexed structure perfect absorbers and one multiplexed structure wideband perfect absorber. The dotted blue curve is the power reflection from a regular nonmultiplexed metal structure perfect absorber with the metal square

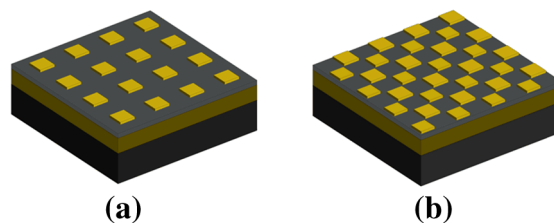


Fig. 1. (Color online) (a) Regular nonmultiplexed perfect light absorber structure and (b) multiplexed perfect light absorber structure.

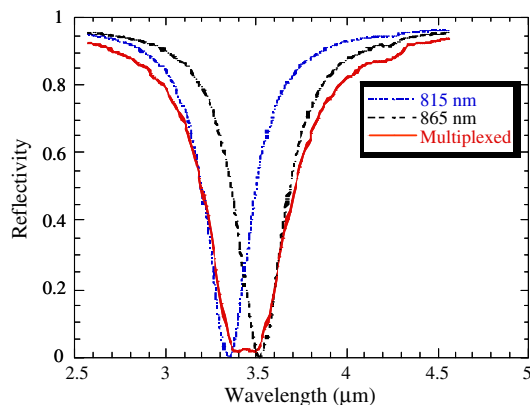


Fig. 2. (Color online) Calculated power reflections from three perfect light absorbers. The dotted blue curve is the power reflection from the perfect absorber structure with one 815 nm gold square in the unit cell. The black dashed curve is the power reflection from the perfect absorber with one 865 nm metal square in the unit cell. The solid red curve is the power reflection from the multiplexed structure perfect absorber with two gold metal squares in the unit cell.

size of 815 nm by 815 nm in the unit cell. Perfect absorption occurs at $3.347 \mu\text{m}$. The reflectivity at this wavelength is 0.16%. The black dashed curve in Fig. 2 is the power reflection from a regular nonmultiplexed structure perfect light absorber with one 865 nm metal square in the unit cell. Perfect absorption occurs at the wavelength of $3.525 \mu\text{m}$. The reflectivity at this wavelength is 0.06%. The solid red curve in Fig. 2 is the power reflection from the multiplexed structure perfect absorber with two gold metal squares in the unit cell. The first gold square is 815 nm by 815 nm. The second gold square is 865 nm by 865 nm. The two metal squares are offset from each other by 210 nm in two dimensions in the unit cell. In all three perfect absorber structures, the gold film thickness is 55 nm and the magnesium fluoride layer thickness is 75 nm. The unit cells in the three perfect absorber structures repeat themselves with the same period of 2100 nm. It is seen clearly from Fig. 2 that the multiplexed structure achieves a much wider near-perfect absorption band than the regular nonmultiplexed structure absorbers.

We calculated the electric field intensity distribution in the middle plane inside the MgF_2 spacing layer (37.5 nm above the surface of the thick gold metal layer) in the unit cell of the multiplexed absorber structure. In the unit cell, the 815 nm gold square is on the bottom left and the 865 nm gold square is on top right. Figure 3(a) shows the electric field intensity distribution calculated at $3.35 \mu\text{m}$, a wavelength on the short side of the wide absorption band. It can be seen that the 815 nm metal square is resonantly excited. Figure 3(b) shows the electric field intensity distribution at the wavelength of $3.395 \mu\text{m}$, the center of the wide absorption band. At this wavelength, both metal squares exhibit strong local field enhancement. Figure 3(c) shows the electric field intensity distribution at the wavelength of $3.45 \mu\text{m}$, on the long wavelength side of the wide absorption band. It can be seen that the 865 nm metal square exhibits strong field enhancement as expected. Figure 3(d) shows the electric field distribution at the wavelength of $4.0 \mu\text{m}$, a wavelength outside of the absorption band. None of the plasmon resonance modes of two gold squares are

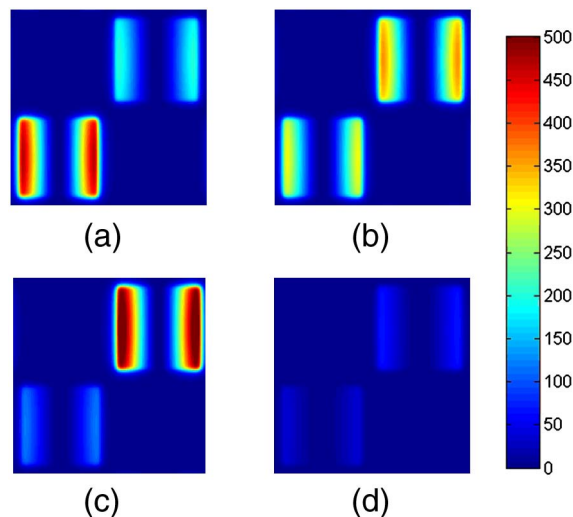


Fig. 3. (Color online) Electric field intensity distributions in the center plane of the MgF_2 spacing layer in the unit cell of the multiplexed absorber structure: (a) electric field intensity distribution at $3.35 \mu\text{m}$ wavelength, (b) electric field intensity distribution at $3.395 \mu\text{m}$ wavelength in the center of the wide absorption band, (c) electric field intensity distribution at $3.45 \mu\text{m}$ wavelength, and (d) electric field intensity distribution at $4.0 \mu\text{m}$, which is outside of the absorption band.

excited. The electric field intensity distributions in Fig. 3 show clearly that the two plasmon resonance modes in the multiplexed structure contribute to the broadening of the absorption band.

We fabricated two nonmultiplexed narrow band perfect light absorbers and one multiplexed structure wide-band perfect light absorber in one fabrication process. The fabrication process started with a polished silicon wafer as the substrate. First, we deposited a 20 nm titanium adhesion layer on the silicon wafer substrate followed by a 250 nm thick gold layer. A 75 nm MgF_2 spacer layer was then deposited on the thick gold layer. After a wet chemical cleaning, PMMA 495K diluted with anisole at a 1:1 ratio was spin coated onto the MgF_2 surface. Electron beam lithography was then used to define three different patterns: an array of 815 nm squares, an array of 865 nm squares, and an array of multiplexed squares of 815 nm and 865 nm in the unit cell. The periods of all three unit cell patterns are the same at 2100 nm. In the multiplexed structure, one gold metal square was offset from the other by 210 nm, horizontally and vertically. The overall size of each fabricated device is $100 \mu\text{m}^2$. Each pattern is placed 5 mm from the others in order to avoid possible cross talk during the subsequent measurement process. After development in a solution of MIBK/IPA, a 3 nm titanium adhesion layer and a 55 nm gold film were evaporated onto the patterned e-beam resist. A standard lift-off process was followed with acetone to remove the areas of unwanted material. Figure 4(a) shows a scanning electron micrograph (SEM) image of the periodically arranged nonmultiplexed 815 nm gold squares. Figure 4(b) shows a SEM image of the multiplexed structure where 815 nm and 865 nm gold metal squares are both included in the unit cell.

We measured the power reflection from three fabricated perfect absorbers using a microscope coupled

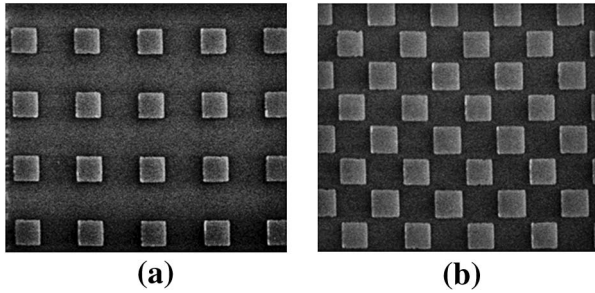


Fig. 4. SEM images of the gold squares in the fabricated perfect light absorbers: (a) regular nonmultiplexed structure including one 815 nm gold square in the unit cell and (b) wideband multiplexed structure including 815 nm and 865 nm gold squares in the unit cell.

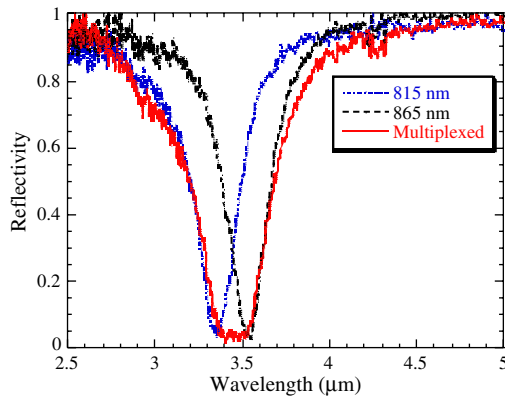


Fig. 5. (Color online) Measured power reflection versus the wavelength from the multiplexed gold metal structure perfect absorber (solid red curve), the nonmultiplexed structure absorber of 815 nm \times 815 nm metal square (dotted blue curve), the nonmultiplexed structure absorber of 865 nm \times 865 nm metal square (dashed black curve) in the unit cells.

Fourier transform IR spectrometer (Bruker Vertex 80V FTIR and Hyperion microscope). A 36 \times reflecting objective lens was used in the microscope, and the signal was detected with a mercury cadmium telluride detector. The microscope field of view was reduced to 50 μm \times 50 μm with the aid of a set of apertures. This allows us to obtain measurements over a more uniform area of the 100 μm^2 patterns because the proximity effect in the lithographic process may cause the patterned metal squares near the periphery of the devices to be undersized.

The power reflection measured from all three perfect absorbers versus the wavelength is plotted in Fig. 5. The dotted blue curve is the power reflection from the regular nonmultiplexed structure perfect absorber with one 815 nm gold square in the unit cell. The device has near-perfect absorption of 96% at the 3.36 μm wavelength. The dashed black curve is the power reflection from the regular nonmultiplexed structure perfect absorber with one 865 nm gold square in the unit cell. This device has near-perfect absorption of 96.7% at the 3.55 μm wavelength. It has a longer near-perfect absorption wavelength because of the larger size of the metal square in the unit cell. The solid red curve in Fig. 5 is the measured power reflectivity from the multiplexed structure perfect absorber with 815 nm and 865 nm gold

metal squares in the unit cell. The multiplexed structure's absorption reaches above 98% over a wide spectral band centered at 3.45 μm wavelength. It can be seen that the multiplexed structure's absorption band has been expanded significantly due to the two gold metal squares of different sizes in the unit cell.

In summary, we have experimentally demonstrated a wideband perfect light absorber using multiplexed metal structures with two plasmon resonance modes in the structure. The multiplexed structure metamaterial surface near-perfectly absorbs above 98% light energy over a wide spectral band centered at the mid-IR wavelength of 3.45 μm . Our experimental results agree well with numerical simulation results. The demonstrated multiplexed structure wideband perfect light absorption concept can be applied for future applications in enhanced optical sensing and imaging.

Junpeng Guo acknowledges the support from the ASEE–Air Force Office of Scientific Research (AFOSR) Summer Faculty Fellowship Program. Joshua Hendrickson acknowledges support from the Air Force Office of Scientific Research (AFOSR) through the program LRIR 10RY04COR. This work was also partially supported by the National Science Foundation (NSF) through the award NSF no. 0814103 and the National Aeronautics and Space Administration (NASA) through grant no. NNX07 AL52A.

References

1. R. W. Wood, *Philos. Mag.* **4**, 396 (1902).
2. A. Hessel and A. A. Oliner, *Appl. Opt.* **4**, 1275 (1965).
3. O. Hunderi and H. P. Myers, *J. Phys F.* **3**, 683 (1973).
4. M. C. Hutley and D. Maystre, *Opt. Commun.* **19**, 431 (1976).
5. E. Popov, L. Tsonev, and D. Maystre, *J. Mod. Opt.* **37**, 379 (1990).
6. E. Popov, L. Tsonev, and D. Maystre, *Appl. Opt.* **33**, 5214 (1994).
7. N. I. Landy, S. Sajuyigbe, J. J. Mock, D. R. Smith, and W. J. Padilla, *Phys. Rev. Lett.* **100**, 207402 (2008).
8. H. Tao, N. I. Landy, C. M. Bingham, X. Zhang, R. D. Averitt, and W. J. Padilla, *Opt. Express* **16**, 7181 (2008).
9. E. Popov, D. Maystre, R. C. McPhedran, M. Neviere, M. C. Hutley, and G. H. Derrick, *Opt. Express* **16**, 6146 (2008).
10. T. V. Teperik, F. J. García de Abajo, A. G. Borisov, M. Abdelsalam, P. N. Bartlett, Y. Sugawara, and J. J. Baumberg, *Nat. Photon.* **2**, 299 (2008).
11. Y. Avitzour, Y. A. Urzhumov, and Gennady Shvets, *Phys. Rev. B* **79**, 033101 (2009).
12. C. Hu, Z. Zhao, X. Chen, and X. Luo, *Opt. Express* **17**, 11039 (2009).
13. X. Liu, T. Starr, A. F. Starr, and W. J. Padilla, *Phys. Rev. Lett.* **104**, 207403 (2010).
14. J. Hao, J. Wang, X. Liu, W. J. Padilla, L. Zhou, and M. Qiu, *Appl. Phys. Lett.* **96**, 251104 (2010).
15. N. Liu, M. Mesch, T. Weiss, M. Hentschel, and H. Giessen, *Nano Lett.* **10**, 2342 (2010).
16. C. Hu, L. Liu, Z. Zhao, X. Chen, and X. Luo, *Opt. Express* **17**, 16745 (2009).
17. J. Guo, Y. Zou, H. Leong, and B. Zhang, in *Photonic Metamaterials and Plasmonics*, OSA Technical Digest (CD) (Optical Society of America, 2010), paper MWB4.
18. A. D. Rakic, A. B. Djuricic, J. M. Elazar, and M. L. Majewski, *Appl. Opt.* **37**, 5271 (1998).
19. M. J. Dodge, *Appl. Opt.* **23**, 1980 (1984).